High-frequency acoustic-phonon generation by heated electrons in parabolic-quantum-well wires in tilted magnetic fields

1996 J. Phys.: Condens. Matter 8 11111

(http://iopscience.iop.org/0953-8984/8/50/034)

J. Phys.: Condens. Matter **8** (1996) 11111–11120. Printed in the UK

High-frequency acoustic-phonon generation by heated electrons in parabolic-quantum-well wires in tilted magnetic fields

W Xu and C Zhang

Department of Physics, University of Wollongong, NSW 2522, Australia

Received 2 July 1996, in final form 29 August 1996

Abstract. We present a detailed theoretical study on high-frequency acoustic- (AC-) phonon generation from a GaAs-based parabolic-quantum-well (PQW) wire system in strong magnetic fields. A situation where the magnetic field is applied perpendicular to the quantum wire but at an angle to the confining potential of the one-dimensional electron gas is taken into account. The frequency and angular distribution of AC-phonon emission has been studied through calculating the electron-energy-loss rate in this configuration. The results obtained from this study indicate that: (1) in the presence of tilted magnetic fields, a PQW wire is a system in which the electron energy spectrum is independent of the angle in which the magnetic field is applied; (2) the frequencies of the AC phonons generated are around $f = \omega_Q/2\pi \sim 10^2$ GHz and depend weakly on the strength and angle of the magnetic field; (3) the AC-phonon generation can be markedly enhanced by magnetic fields over all angle regimes; and (4) the AC-phonon emission in tilted magnetic fields has a different dependence on the phonon emission angle from that at zero magnetic field.

1. Introduction

In recent years, it has been realized that GaAs-based low-dimensional semiconductor systems (LDSSs) can be applied as high-frequency acoustical devices such as high-frequency ultrasonic generators [1–6]. The physical mechanism underlying this proposal is based on the generation of high-frequency acoustic (AC) phonons by heated electrons in the device systems. In a LDSS, the conducting electrons are confined within the nanometre distance scale so that the electronic subband energy, the electron kinetic energy, the Fermi energy, etc, are on the meV scale and that the energy transfer during the electronic transitions, due to scattering, etc, can reach the meV scale. Consequently, the energy (frequency) of the AC phonons generated from LDSSs can be on the meV (terahertz, THz) scale.

At present, there are some technical difficulties in detecting experimentally the frequency and angular dependence of the AC-phonon emission, especially in the THz phonon frequency regime. Theoretical calculations and analyses play an important role in designing possible devices and in understanding and predicting the experimental findings. Important contributions have already been made by some authors [2, 3, 5, 6]. The frequency and angular distribution of AC-phonon emission from AlGaAs/GaAs-based two-dimensional semiconductor systems (2DSSs) at zero [2] and strong magnetic fields applied parallel [6] and perpendicular [5] to the interface of the 2DSSs has been studied in detail over the last two decades. The AC-phonon emission from quantum wire systems has received great attention recently [3] due to the distinctive features of electron–phonon interactions in these

0953-8984/96/5011111+10$19.50

novel systems. The important and unusual natures of the electronic subband structure and the electronic properties for a one-dimensional electron system (1DES) have been summarized by, e.g., reference [7]. In this paper, we will look at the AC-phonon generation from a quantum wire system in strong magnetic fields. In order to find out the condition for being able to detect the strongest phonon signal, we consider the situation where the magnetic field is applied at an angle to the confining potential of the 1DES. The electronic subband structure in this configuration is studied in section 2. From both a fundamental study and a device application points of view, the most important theoretical result which will help experimental measurements is the intensity of AC-phonon emission as a function of phonon frequency and phonon emission angle. In section 3, we study the frequency and angular distribution for AC-phonon emission by heated electrons in a 1DES in tilted magnetic fields via calculating the electron-energy-loss rate caused by electron–AC-phonon interaction. The numerical results obtained from the present study are presented and discussed in section 4, where we can see some unusual and interesting features of AC-phonon emission in the defined configuration. The conclusions of this study are summarized in section 5.

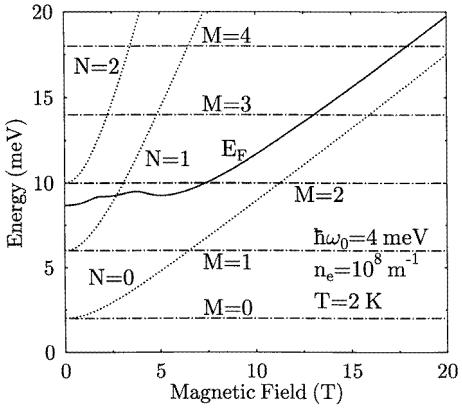

Figure 1. The electronic subband energy $\varepsilon_{MN} = (M + 1/2)\hbar\omega_0 + (N + 1/2)\hbar\omega_B$ and Fermi energy E_F in a parabolic-quantum-well wire as a function of the magnetic field. ε_{MN} does not depend on the angle of the magnetic fields applied. n_e is the electron density for the 1DEG and ω_0 is the characteristic frequency defining a PQW wire system.

2. Electronic subband structure for a parabolic-quantum-well wire in tilted magnetic fields

The basic difference of phonon emission and scattering by a one-dimensional electron gas (1DEG) at zero and strong magnetic fields results from the fact that the electron wave function, electronic energy spectrum and the density of states (DOS) in a strong magnetic field are different from those at $B = 0$. Further, for a 1DEG subjected to a magnetic field, the electronic subband structure will be strongly modified by the strength and angle of the magnetic field, due to the coupling of the magnetic potential to the confining potential of the 1DEG. In this paper, we consider a configuration in which: (1) the quantum wire is along the y-direction; (2) the magnetic field is applied perpendicular to the quantum wire but at an angle to the confining potential of the 1DEG—defining the angle between the magnetic field applied and the x-axis as θ_B, we have $\boldsymbol{B} = B(\cos\theta_B, 0, \sin\theta_B)$; and (3) the confining potential of the 1DEG is modelled by a parabolic-quantum-well (PQW) potential

(or harmonic potential), i.e., $U(x,z) = m_0^*\omega_0^2(x^2+z^2)/2$ where m_0^* is the effective electron mass and ω_0 is the characteristic frequency for the confinement. A PQW wire system can be formed by, e.g., using nanoscale lithographic techniques [8] and/or placing control gate electrodes on the top of a buried GaAs layer [9]. These techniques are usually applied to form the quantum dot structures when an external confinement potential is present along the y-direction. After taking into account the above remarks and using the Landau gauge, i.e., the vector potential $\boldsymbol{A} = B(0, x\sin\theta_B - z\cos\theta_B, 0)$, the free-electron Hamiltonian for a PQW wire in tilted magnetic fields within a single-particle approximation is given by

$$H = -\frac{\hbar^2}{2m_0^*}\frac{\partial^2}{\partial x^2} - \frac{\hbar^2}{2m_0^*}\frac{\partial^2}{\partial z^2} + U(x,z) + \frac{m_0^*}{2}\omega_c^2(l^2k_y + x\sin\theta_B - z\cos\theta_B)^2 \tag{1a}$$

with $l = (\hbar/eB)^{1/2}$ the radius of the ground cyclotron orbit and $\omega_c = eB/m_0^*$ the cyclotron frequency. Using the point canonical transformation, i.e., $X = x\cos\theta_B + z\sin\theta_B$ and $Z = -x\sin\theta_B + z\cos\theta_B - (\omega_c/\omega_B)l_B^2k_y$, the Hamiltonian becomes

$$H = -\frac{\hbar^2}{2m_0^*}\frac{\partial^2}{\partial X^2} + \frac{m_0^*}{2}\omega_0^2X^2 - \frac{\hbar^2}{2m_0^*}\frac{\partial^2}{\partial Z^2} + \frac{m_0^*}{2}\omega_B^2Z^2 + \frac{\hbar^2k_y^2}{2m_B^*} \tag{1b}$$

which represents two harmonic oscillators. Here, we have defined: (i) $\omega_B = \sqrt{\omega_c^2+\omega_0^2}$, $\omega_B = \omega_0$ at $B = 0$; (ii) $l_B = (\hbar/m_0^*\omega_B)^{1/2}$, $l_B = l_0 = (\hbar/m_0^*\omega_0)^{1/2}$ at $B = 0$; and (iii) $m_B^* = m_0^*[1 + (\omega_c/\omega_0)^2]$. The electron wave function and energy spectrum are obtained respectively as

$$|k_y, M, N\rangle = (2^{M+N}M!N!\pi l_0 l_B)^{-1/2}\mathrm{e}^{\mathrm{i}k_y y}\mathrm{e}^{-(\xi_0^2+\xi_B^2)/2}H_M(\xi_0)H_N(\xi_B) \tag{2}$$

with $\xi_0 = X/l_0$, $\xi_B = Z/l_B$ and $H_N(x)$ the Hermite polynomials, and

$$E_{MN}(k_y) = \frac{\hbar^2k_y^2}{2m_B^*} + \left(M+\frac{1}{2}\right)\hbar\omega_0 + \left(N+\frac{1}{2}\right)\hbar\omega_B. \tag{3}$$

Further, from the electronic energy spectrum, the density of states (DOS) for electron in the energy level $\alpha = (M, N)$ is obtained as

$$D_\alpha(E) = \frac{g_s}{2\pi}\sqrt{\frac{2m_B^*}{\hbar^2}}\frac{\Theta(E-\varepsilon_\alpha)}{\sqrt{E-\varepsilon_\alpha}} \tag{4}$$

where $g_s = 2$ accounts for spin degeneracy, $\Theta(x)$ is the unit step function, and

$$\varepsilon_\alpha = (M+1/2)\hbar\omega_0 + (N+1/2)\hbar\omega_B. \tag{5}$$

Comparing equations (2)–(5) with the results obtained from a PQW wire at zero magnetic field, we see that: (1) in the presence of a magnetic field, the electron wave function is described by two coupled harmonic oscillators; (2) the centre of the harmonic-oscillator wave function is shifted by the *strength* of the magnetic field due to the cyclotron motion of the electron; (3) the electronic subband energy ε_α depends only on the strength of the magnetic field; (4) the energy separation between different quantum states (described by $N = 0, 1, 2, \ldots$) and the effective electron mass along the y-direction are enhanced by the magnetic field; and (5) the representative density-of-states effective electron mass is also enhanced by the magnetic field. Nevertheless, for a PQW wire system, the presence of the tilted magnetic field will not change the 1D nature of the electronic system. The electronic subband energy and the chemical potential (or Fermi energy) for a PQW wire are plotted

in figure 1 as a function of the strength of the magnetic field, where the Fermi energy E_F is determined by using the condition of electron number conservation

$$n_e = \frac{1}{\pi}\sqrt{\frac{2m_B^*}{\hbar^2}}\sum_{\alpha}\int_0^{\infty}\frac{\mathrm{d}x}{\sqrt{x}}f^0(x+\varepsilon_\alpha). \tag{6}$$

Here n_e is the electron density of the 1DEG and $f^0(x) = [\mathrm{e}^{(x-E_F)/k_BT}+1]^{-1}$ the Fermi–Dirac function.

3. Acoustic-phonon emission from PQW wires in tilted magnetic fields

Using the Boltzmann equation approach, the average energy-loss rate of an electron to the lattice, due to the electron–phonon interactions in a 1DEG, can be defined by [10]

$$P_T = A\sum_{\alpha}\int \mathrm{d}k_y\ E_\alpha(k_y)\left[\frac{\partial f_\alpha(k_y)}{\partial t}\right]_{coll} = A\sum_{\alpha}\int \mathrm{d}k_y\ f_\alpha(k_y)\left[-\frac{\mathrm{d}\varepsilon}{\mathrm{d}t}\right]_{coll} \tag{7}$$

where $\alpha = (M, N)$, $f_\alpha(k_y)$ is the distribution function for electrons in a state $|k_y, \alpha\rangle$ and $A = [\sum_\alpha \int \mathrm{d}k_y\ f_\alpha(k_y)]^{-1}$ is a normalization factor for which after using the condition of electron number conservation we have $A = 1/(\pi n_e)$. In equation (7), $\partial f_\alpha(k_y)/\partial t$ is the variation of $f_\alpha(k_y)$ at time t by the scattering (collision) process while the variation of electron energy at time t by scattering process is in the form

$$\left[-\frac{\mathrm{d}\varepsilon}{\mathrm{d}t}\right]_{coll} = \frac{g_s}{2\pi}\sum_{\alpha'}\int \mathrm{d}k'_y\ [1-f_{\alpha'}(k'_y)][E_\alpha(k_y)-E_{\alpha'}(k'_y)]W_{\alpha'\alpha}(k'_y,k_y). \tag{8}$$

Here the transition rate for scattering an electron from a state $|k_y, \alpha\rangle$ to a state $|k'_y, \alpha'\rangle$ is given by

$$W_{\alpha'\alpha}(k'_y,k_y) = W^-_{\alpha'\alpha}(k'_y,k_y) + W^+_{\alpha'\alpha}(k'_y,k_y) \tag{9a}$$

and after using Fermi's golden rule

$$W^{\pm}_{\alpha'\alpha}(k'_y,k_y) = \frac{2\pi}{\hbar}\sum_{q_x,q_z}\begin{bmatrix} N_Q \\ N_Q+1\end{bmatrix}C_i(\boldsymbol{Q})G_{\alpha'\alpha}(\boldsymbol{Q})\delta_{k'_y,k_y+q_y}\delta[E_{\alpha'}(k'_y)-E_\alpha(k_y)\mp\hbar\omega_Q]. \tag{9b}$$

Here, the upper (lower) case refers to absorption (emission) of a phonon with energy $\hbar\omega_Q$, $\boldsymbol{Q} = (q_x, q_y, q_z)$ is the phonon wave vector, $N_Q = [\mathrm{e}^{\hbar\omega_Q/k_BT}-1]^{-1}$ is the phonon occupation number, and $C_i(\boldsymbol{Q})$ is the coefficient describing electron interactions with the ith phonon mode. Further, $G_{\alpha'\alpha}(\boldsymbol{Q}) = |\langle M', N'|\mathrm{e}^{\mathrm{i}(q_x x+q_z z)}|M, N\rangle|^2$ is the form factor for electron–phonon interaction. Using the electron wave function for a PQW wire subjected to a tilted magnetic field, we have $G_{\alpha'\alpha}(\boldsymbol{Q}) = C_{M',M}(a^2/2)C_{N',N}((b^2+c^2)/2)$ where $a = l_0(q_x\cos\theta_B + q_z\sin\theta_B)$, $b = l_B(q_x\sin\theta_B - q_z\cos\theta_B)$, $c = (\omega_c/\omega_B)l_Bq_y$, and $C_{N,N+J}(y) = [N!/(N+J)!]\mathrm{e}^{-y}y^J[L_N^J(y)]^2$ with $L_N^J(y)$ being the associated Laguerre polynomials. For a PQW wire in tilted magnetic fields, the form factor for the electron–phonon interaction depends on q_x, q_y and q_z.

To investigate the frequency and angular distribution of AC-phonon emission in the geometry defined in this study, it is convenient to define the phonon wave vector in polar coordinates: $\boldsymbol{Q} = Q(\sin\phi\cos\theta, \cos\phi, \sin\phi\sin\theta)$ where ϕ is the polar angle and the polar axis is taken along the direction of the quantum wire. θ and ϕ also define the phonon emission angle. In this paper, we use a Fermi–Dirac type of statistical energy distribution function as the electron distribution, through $f_\alpha(k_y) = f(E_\alpha(k_y))$,

where $f(x) = [e^{(x-E_F)/k_BT_e} + 1]^{-1}$ with T_e being the electron temperature. The inclusion of electron–phonon scattering in the case of degenerate statistics implies that phonon emission occurs mainly among the occupied electronic subbands accompanied by electronic transitions around the Fermi level. Thus, the total electron-energy-loss rate (EELR) per electron is in the form

$$P_T = \int_0^\infty d\omega_Q \int_0^{2\pi} d\theta \int_0^\pi d\phi \; P(\omega_Q, \theta, \phi) \tag{10}$$

where we have used the long-wavelength approximation for AC-phonon modes, i.e., $\omega_Q \simeq v_i Q$ with v_i the corresponding sound velocity. The frequency and angular distribution function for the phonon emission is given by

$$P(\omega_Q, \theta, \phi) = \sum_{\alpha', \alpha} [(N_Q + 1) I^-_{\alpha'\alpha}(\boldsymbol{Q}) - N_Q I^+_{\alpha'\alpha}(\boldsymbol{Q})] \tag{11}$$

and

$$I^\pm_{\alpha'\alpha}(\boldsymbol{Q}) = \frac{m_B^* Q \omega_Q}{2\pi^3 \hbar^2 v_i n_e} C_i(\boldsymbol{Q}) G_{\alpha'\alpha}(\boldsymbol{Q}) f(\varepsilon_\alpha + \varepsilon^\pm_{\alpha'\alpha})[1 - f(\varepsilon_\alpha + \varepsilon^\pm_{\alpha'\alpha} \pm \hbar\omega_Q)] \tan\phi \tag{12}$$

where $\varepsilon^\pm_{\alpha'\alpha} = (\varepsilon_\alpha - \varepsilon_{\alpha'} - \varepsilon_{q_y} \pm \hbar\omega_Q)^2 / 4\varepsilon_{q_y}$ with $\varepsilon_{q_y} = \hbar^2 q_y^2 / 2m_B^*$. Equation (11) indicates that the net energy transfer rate is the difference between phonon emission and absorption by heated electrons in the device system.

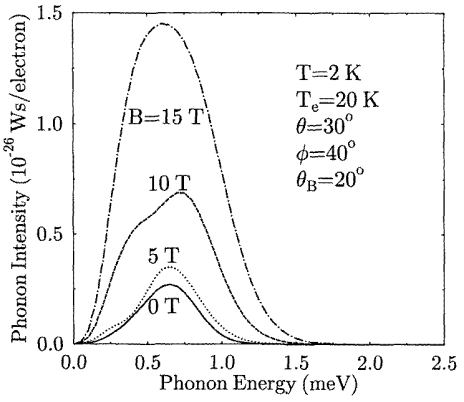

Figure 2. The acoustic-phonon spectrum detected at a fixed angle (θ, ϕ) for different magnetic fields applied at a fixed angle θ_B to the x-axis. The quantity $P(\omega_Q, \theta, \phi)$ is presented and T_e is the electron temperature. The sample parameters are as shown in figure 1.

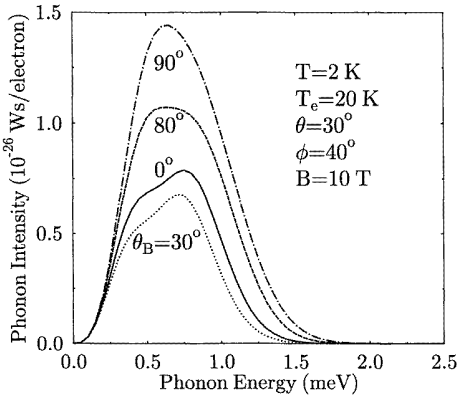

Figure 3. The acoustic-phonon spectrum, $P(\omega_Q, \theta, \phi)$, detected at a fixed angle (θ, ϕ) and at a magnetic field $B = 10$ T applied at different angles to the x-axis. The sample parameters are as shown in figure 1.

For a GaAs-based PQW wire structure, the phonon modes in the device system are very similar to those in GaAs. The results obtained from experimental [1] and theoretical [6] studies have indicated that for GaAs-based LDSSs at intermediate excitation levels (i.e., within the electron temperature range $10 < T_e < 40$ K), the electron–AC-phonon interactions are mainly via coupling with deformation-potential acoustic phonons. When $T_e < 10$ K ($T_e > 40$ K), electron interaction with piezoelectric phonons (optic phonons) is a major mechanism for the energy relaxation of the excited electrons. In the present study, we limit ourselves to the situation where AC-phonon emission is generated mainly via electron interactions with the deformation-potential acoustic phonons. For GaAs only

the longitudinal-AC-phonon mode is connected with the deformation potential (DP) and the coupling coefficient is given by

$$C_{DP}(\boldsymbol{Q}) = \frac{\hbar E_D^2 Q}{2\rho v_l} \tag{13}$$

where E_D is the deformation-potential constant ($E_D \simeq 11$ eV for GaAs-based LDSSs), ρ is the density of the material ($\rho = 5.37$ kg m^{-3} for GaAs), and v_l is the longitudinal sound velocity ($v_l = 5.29 \times 10^7$ m s^{-1} for GaAs). Introducing the coupling coefficient (equation (13)) into equation (12), we can perform numerical calculations for AC-phonon emission via electron interaction with deformation-potential acoustic phonons.

4. Results and discussion

In this paper, our calculations are performed for GaAs-based PQW wires. The effective electron mass for GaAs at zero magnetic field is $m_0^* = 0.0665m_e$ where m_e is the electron rest mass. The sample parameters, such as the characteristic frequency of a PQW and the electron density of the 1DEG, can be taken from the experimental data. For a model calculation, we take $\hbar\omega_0 = 4$ meV and $n_e = 10^8$ m^{-1}.

Normally the AC-phonon emission can be detected by, e.g., phonon emission experiments [11] which are carried out at low temperatures using superconducting bolometers as phonon detectors. In the calculation, we take the lattice temperature $T = 2$ K which depends on using an Al bolometer as the detector [1]. We take the electron temperature as $T_e = 20$ K in the calculations, which corresponds to an excitation energy around about 1 pW per electron according to reference [1].

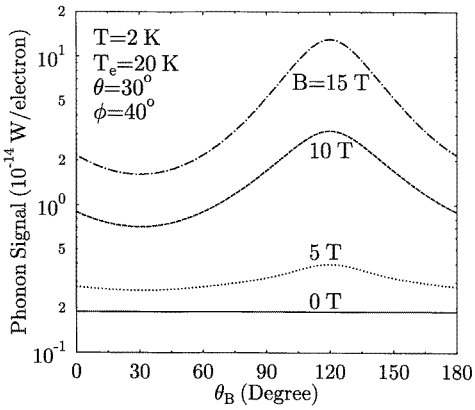

Figure 4. The total intensity of the phonon signal detected at a fixed angle (θ, ϕ) as a function of the angle of the magnetic field applied for different strengths of the magnetic field. The quantity $P(\theta, \phi) = \int_0^\infty \mathrm{d}\omega_Q \; P(\omega_Q, \theta, \phi)$ is presented and the sample parameters are the same as in figure 1.

The spectrum of the AC phonons generated is shown in figures 2 and 3 where we plot the quantity $P(\omega_Q, \theta, \phi)$ as a function of phonon frequency. We note that: (i) the frequency of the AC phonons generated from a PQW wire in magnetic fields is around $\omega_Q/2\pi \sim 10^{11}$ Hz $= 10^2$ GHz (see figures 2 and 3); (ii) AC-phonon generation is markedly enhanced by the magnetic field (see figure 2). The intensity of phonon emission increases

with B (also see figure 5, later); and (iii) the angle of the magnetic field applied has a strong influence on the intensity of phonon signal detected but affects weakly the phonon frequency (see figure 3). The most significant conclusion that we draw from these results is that a pronounced enhancement of AC-phonon generation can be achieved by applying a magnetic field to a PQW wire structure without varying significantly the intrinsic features of the generator at zero magnetic field.

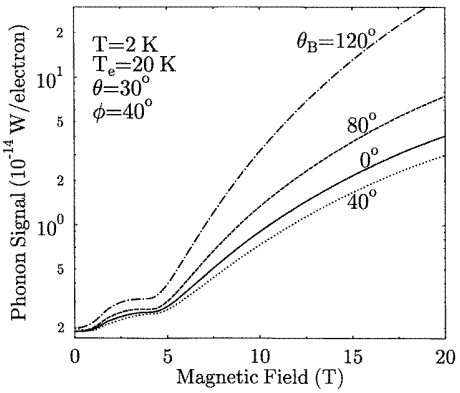

Figure 5. The total intensity of the phonon signal, $P(\theta, \phi)$, detected at a fixed angle (θ, ϕ) as a function of magnetic field applied at different angles to the x-axis. The sample parameters are as shown in figure 1.

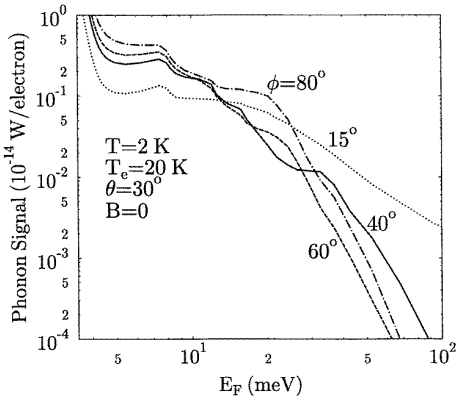

Figure 6. The total intensity of the phonon signal, $P(\theta, \phi)$ detected at a fixed angle θ for different angles ϕ, as a function of Fermi energy at zero magnetic field. The Fermi energy is changed by varying the electron density from about 10^5–10^{10} m^{-1}.

The dependence of the total intensity of AC-phonon signals detected at a fixed angle (θ, ϕ) (i.e., the quantity $P(\theta, \phi) = \int_0^\infty \mathrm{d}\omega_Q \; P(\omega_Q, \theta, \phi)$) on the angle of the magnetic field applied is shown in figure 4 for different magnetic field strengths. A stronger dependence of the phonon emission on θ_B can be found for a larger magnetic field, due to the fact that the detected AC-phonon signals increase with increasing B (see figure 5). The strongest AC-phonon emission can be detected at around $\theta_B = 120^\circ$. The results obtained from our further calculations indicate that this phenomenon can be observed over all phonon emission angles. Hence, we conclude that for a PQW wire the strongest AC-phonon emission can be generated by applying a magnetic field at an angle $\theta_B = 120^\circ$ to the x-axis of the device system. We note that the usage of equation (13) implies that we may take the (001) direction of a crystal with zinc-blende symmetry (such as GaAs) as the z-direction in our defined configuration. In figure 5, the increase in the phonon generation with increasing magnetic field is induced mainly by an enhancement of the effective electron–phonon interaction caused by enhanced effective electron mass and density of states in high magnetic fields and by a magnetic-field-modulated Fermi energy (see figure 1). The strong dependence of phonon generation on the Fermi energy is evident in figure 6 where we plot the intensity of the phonon signal as a function of Fermi energy at $B = 0$. The inclusion of electron–phonon scattering in the case of degenerate statistics requires phonon generation to be accompanied by electronic transitions around the Fermi level. Therefore, a variation in Fermi energy will result in a variation of scattering channels for phonon emission.

The AC-phonon emission angle in a PQW wire in tilted magnetic fields is shown in figures 7 and 8. The angular distribution of phonon generation is determined by: (i) the requirements of momentum and energy conservations during electron–phonon scattering

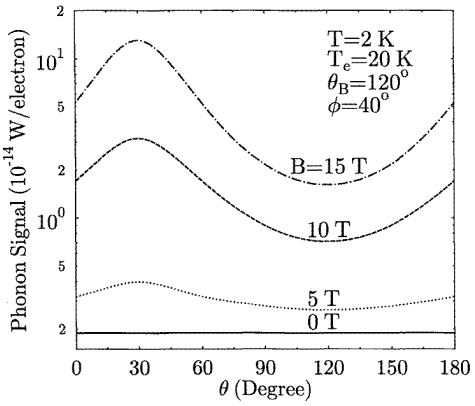

Figure 7. The dependence of acoustic-phonon emission on the angle θ at a fixed angle ϕ for different magnetic fields applied at a fixed angle θ_B to the x-axis. $P(\theta, \phi)$ is presented and the sample parameters are as shown in figure 1.

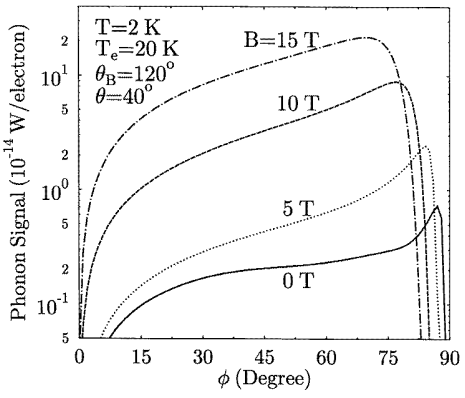

Figure 8. The dependence of acoustic-phonon emission on the angle ϕ at a fixed angle θ for different magnetic fields applied at a fixed angle θ_B to the x-axis. $P(\theta, \phi)$ is presented and the sample parameters are as shown in figure 1.

events; (ii) the electron–phonon interaction matrix element, i.e., $C_i(\boldsymbol{Q})$. For electron interactions with deformation-potential acoustic phonons, $C_{DP}(\boldsymbol{Q})$ is independent of the phonon emission angle (see equation (13)); and (iii) the form factor for electron–phonon interactions. For a PQW wire at $B = 0$, the form factor depends only on $q_x^2 + q_z^2$ (i.e., on the angle ϕ) and a weak dependence of the phonon emission on the angle θ can be expected (see figure 7). When $B \neq 0$ the form factor is a function of q_x, q_y and q_z, which results in a strong dependence of the phonon emission on the angle θ and on the strength and angle of the magnetic field applied. The nature of electron interactions with bulk-like AC phonons implies that the form factor depends always on q_x and q_z. Therefore, a strong dependence of AC-phonon emission on the angle ϕ can be observed in all magnetic fields (see figure 8). The results obtained from our further calculations show that the dependence of AC-phonon generation on the phonon emission angle differs slightly on varying the angle of the magnetic fields applied. This is due to the fact that the form factor for electron–phonon interaction depends on θ_B.

5. Summary

In this paper, we have studied the electronic subband structure for a parabolic-quantum-well wire system in the presence of a magnetic field applied perpendicular to the quantum wire but at an angle to the confining potential of the 1DES. We have found that: (1) the electron energy spectrum and the effective electron mass in this configuration depend only on the strength of the magnetic field applied; (2) the effective electron mass and the representative density-of-states effective electron mass are enhanced by the magnetic field; and (3) the Fermi energy in the electronic system depends strongly on the magnetic field applied. Nevertheless, the electrons in a PQW wire in tilted magnetic fields still retain their 1D nature. An enhanced effective electron mass and density of states in high magnetic fields will lead to an enhancement of the effective electron–phonon interaction. Together with a strong dependence of the Fermi energy on the magnetic field, consequently, the generation of high-frequency acoustic phonons will be enhanced at high magnetic fields through intra-

and inter-subband electronic transitions.

We have developed a theoretical model which can be used to calculate the frequency and angular distribution of acoustic-phonon emission from a PQW wire in strong magnetic fields. Considering that in the intermediate-electron-temperature regime ($10 < T_e < 40$ K) AC-phonon emission is generated mainly through electron interactions with deformation-potential acoustic phonons, we have studied the dependence of AC-phonon emission on the phonon frequency, phonon emission angle, and on the strength and angle of the magnetic field applied. The results obtained from this theoretical study have shown that: (1) for a PQW wire subjected to magnetic fields, the frequency of the AC phonons generated is around $\omega_Q/2\pi \sim 10^{11}$ Hz; (2) the generated phonon frequency depends weakly on the strength and angle of the applied magnetic fields; (3) the generation of AC phonons increases rapidly with increasing magnetic field; (4) the strongest phonon emission can be generated at $\theta_B = 120^\circ$ for a fixed strength of the magnetic field over all phonon emission angles; and (5) for a PQW wire structure, the AC-phonon emission angle in tilted magnetic fields differs from that at $B = 0$ and depends on the strength and angle of the applied magnetic fields.

The application of GaAs-based low-dimensional electron systems to electronic, photonic and optoelectronic devices has been investigated rather intensively over the past two decades. The exploration of using these novel systems as high-frequency acoustical devices, such as high-frequency ultrasonic generators, through generating high-frequency acoustic phonons by electrically heated electrons in the device systems, will enhance the field of device applications, and is the motivation behind this study. The theoretical results presented in this paper may help in the detection of acoustic-phonon emission by, e.g., phonon emission experiments.

Acknowledgment

This work was supported by the Australian Research Council.

References

[1] For experimental work for a 2DSS at zero magnetic field, see
Hawker P, Kent A J, Hauser N and Jagadish C 1995 *Semicond. Sci. Technol.* **10** 601
Hawker P, Kent A J, Hughes O H and Challis L J 1992 *Semicond. Sci. Technol.* **7** B29

[2] For theoretical work for a 2DSS at zero magnetic field, see, e.g.,
Vasko F T and Mitin V 1995 *Phys. Rev.* B **52** 1500
Vasko F T, Balev G and Vasilopous P 1993 *Phys. Rev.* B **47** 16 433
Xu W and Mahanty J 1994 *J. Phys.: Condens. Matter* **6** 6265
Fal'ko I and Iordanskii S V 1992 *J. Phys.: Condens. Matter* **4** 9201
Benedict K A 1992 *J. Phys.: Condens. Matter* **4** L371

[3] For theoretical work for a 1DSS at zero magnetic field, see, e.g.,
Mickevičius R and Mitin V 1995 *Phys. Rev.* B **51** 1609
Mickevičius R, Mitin V, Kochelap V, Stroscio M A and Iafrate G J 1995 *J. Appl. Phys.* **77** 5095
Xu W 1996 *Appl. Phys. Lett.* **68** 1353

[4] For experimental work for a 2DSS in perpendicular magnetic fields, see
Hawker P, Kent A J, Challis L J, Henini M and Hughes O H 1989 *J. Phys.: Condens. Matter* **1** 1153
Kent A J, Rampton V W, Newton M I, Carter P J A, Hardy G A, Hawker P, Russell P A and Challis L J 1988 *Surf. Sci.* **196** 410
Challis L J 1995 *Physica* B **204** 117

[5] For theoretical work for a 2DSS in perpendicular magnetic fields, see
Benedict K A 1991 *J. Phys.: Condens. Matter* **3** 1279
Badalian S M and Levinson Y B 1991 *Phys. Lett.* **155A** 200

Toombs G A, Sheard F W, Neilson D and Challis L J 1987 *Solid State Commun.* **64** 577
[6] For theoretical work for a 2DSS in parallel magnetic fields, see
Xu W and Zhang C 1996 *Appl. Phys. Lett.* **68** 823
Xu W 1996 *Phys. Rev.* B **54** 2775
[7] Li Q P and Das Sarma S 1991 *Phys. Rev.* B **43** 11 768
[8] See, e.g.,
Cheung R, Thoms S, Watt M, Foad M A, Sotomayor Torres C M , Wilkinson C D W, Cox U J, Cowley R A, Dunscombe C and Williams R H 1992 *Semicond. Sci. Technol.* **7** 1189
[9] See, e.g.,
Gumbs G, Huang D, Qiang H, Pollak F H, Wang P D, Sotomayor Torres C M and Holland M C 1994 *Phys. Rev.* **B 50** 10 962
[10] Seeger K 1982 *Semiconductor Physics (Springer Series in Solid-State Sciences 40)* (New York: Springer)
[11] Challis L J, Kent A J and Rampton V W 1990 *Semicond. Sci. Technol.* **5** 1179
Narayanamurti V 1981 *Science* **213** 717
Hensel J C, Dynes R C and Tsui D C 1983 *Phys. Rev.* B **28** 1124
Rothenfusser M, Köster L and Dietsche W 1986 *Phys. Rev.* B **34** 5518